

INNER MECHANISMS OF FLUX TRANSFER EVENTS OBSERVED BY CLUSTER

H. Khan^(1,2), H. Laakso⁽²⁾, M. Dunlop⁽³⁾, M.G.G.T. Taylor⁽²⁾, C.P. Escoubet⁽²⁾, H. Opgenoorth⁽²⁾, A. Masson⁽²⁾

⁽¹⁾*Mullard Space Science Laboratory, University College London, Holmbury St Mary, Dorking, UK*

⁽²⁾*ESA/ESTEC, Keplerlaan 1, 2200 AG Noordwijk ZH, The Netherlands*

⁽³⁾*Space Science and Technology Dept, Rutherford Appleton Laboratory, Didcot, Oxon., UK*

ABSTRACT

On the 6th April 2004, Cluster made a high-latitude outbound pass of the magnetopause. During this time, FTE-like signature were observed in several of the Cluster data sets, including the magnetic field experiment (FGM) and the electric field and drift velocities (EFW). Since the EFW data set can be resolved to 25Hz data, the features were investigated further to highlight the substructures observed. Each FTE was formally identified using the boundary normal coordinate transformation of the FGM data, and corresponded with density depletions in the EFW data, and enhancements in the drift velocities within key regions. Magnetic field and plasma rotations were observed at the leading and trailing edges of the FTE which can be attributed to the skewing of the field due to reconnection and the significant dawnward IMF B_y . The flow was directed in accordance with the field tension force pulling the flux tubes and plasma in a eastward rotation away from the reconnection site. The exterior magnetosheath plasma was oriented poleward and westward, thus creating a rotational discontinuity upon crossing into the FTE structure. This was confirmed by a positive result in the Walen test for each of the events. Large rotations in the flow were also observed in the core region of the FTEs and this may be associated with the motion of the newly reconnected material within the FTE.

1. INTRODUCTION

Magnetic reconnection, first envisaged by [1] has repeatedly been shown to be an effective mechanism for transferring energy, momentum and plasma from the solar wind into the magnetosphere (e.g [2]). The dynamics of the reconnection process are known to modulate with the orientation and strength of the interplanetary magnetic field (IMF) and the solar wind conditions (e.g [3]) with the most active periods occurring when the interplanetary magnetic field (IMF) is oriented southward ($-B_z$). Under such condition, low-latitude subsolar reconnection is instigated, which has been observed to occur in both a continuous, quasi-steady rate (e.g. [4], [5]) or in a more transient, impulsive manner (eg. [6]). The pulsed nature was characterised as discrete bursts of reconnection leading to the ripping of flux tubes from the magnetosphere and

convecting downtail. [7] and [8] offered a detailed description of these events, and coined the term ‘flux transfer events’ (FTE) for these signatures. Since the initial observations of FTEs, a great deal of research into the properties and structures of these events has been carried out (e.g. [9], [10], [11]). Traditionally the most common signatures used to initially highlight FTEs is the bipolar oscillation in the magnetic field component normal to the magnetopause boundary. Further studies showed the discrete plasma populations within FTEs to be of both magnetosheath and magnetospheric origin (e.g. [12]). Detailed studies of the reconnection mechanisms have allowed the overall structure and dynamics of FTEs to be exposed, however there is a great deal of internal motion and turbulence that has thus far not been exposed. [13] investigated FTE signatures using the Cluster multi-spacecraft and were able to ascertain distinct differences between the 4 satellite plasma observations leading to a hypothesis that there was a certain amount of redistribution of flux tubes within the FTEs. They suggested that there was a recirculation of older flux tubes carrying magnetosheath electrons from the leading edge of the FTE along the Earthward boundary, set in motion by some form of drag. This leads to a population of magnetosheath electrons on the Earthward edge of the FTE formed by the motion of those old reconnected flux tubes.

In this paper, we present Cluster observations using high time resolution Electric Fields and Waves (EFW) data and Fluxgate Magnetometer (FGM) data as the spacecraft crossed the high-latitude magnetopause boundary during a period of ongoing reconnection. We pay particular attention to the transient reconnection (FTE) signatures observed and look in detail at the drifts and electric fields associated with each event. The four spacecraft configuration is utilised to understand the current configuration as the FTEs traverse the satellites. In the following section, upstream solar wind conditions are presented together with the Cluster data sets. In section 3 these data sets will be discussed in the context with our understanding of the plasma environment as well as comparing with previous studies. Finally the results and conclusions will be presented in section 4.

2. OBSERVATIONS

2.1 Cluster orbit configuration

The four Cluster spacecraft [14] were in tetrahedral configuration travelling outbound of the magnetosphere during the time interval 0400-0530 UT on the 6th April 2004. Figure 1 shows the spacecraft orbit in XZ plane (left) and the YZ plane (right) for this time interval relative to a model magnetosphere using the actual upstream IMF and solar wind conditions observed by the Advanced Composition Explorer (ACE). Cluster crossed the magnetopause boundary at high-latitudes in the pre-noon at ~0434 UT (see Fig. 3). The interspacecraft distance was only ~300 km so all satellites observed the boundary in quick succession. Model magnetic field lines are also plotted using the T96 model illustrating that the cusp crossing during this interval. The details of the crossing are apparent in the data sets described below.

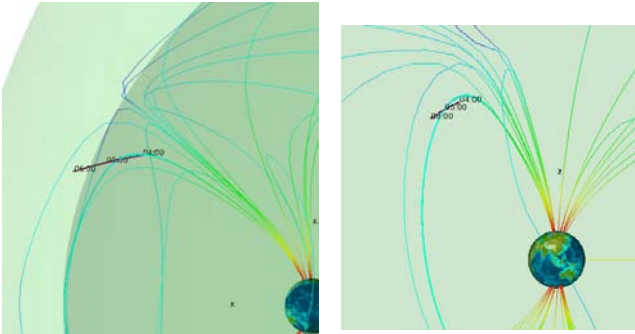


Figure 1. Orbital path of Cluster spacecraft on 6th April 2004 between 0400-0600 UT in XZ (left) and YZ (right) planes. A model magnetopause and bow shock are also shown using current IMF conditions, together with magnetospheric field lines from T96.

2.2 Upstream Solar Wind Conditions

On the 6th April 2004 from 0400-0530 UT, whilst the Cluster spacecraft made an outbound pass through the magnetosphere into the magnetosheath, the upstream solar wind and IMF conditions as observed by the ACE [15] are shown in Figure 2. The top four panels show the three components of the magnetic field in GSM coordinates as measured by the Magnetic Field Experiment (MFE) [16] together with the total field strength, B_T . The subsequent panel gives the IMF clock angle, where 0 degrees indicates a purely northward IMF. Finally the bottom three panels present the solar wind density, velocity and dynamic pressure, respectively from the Solar Wind Electron Proton Monitor (SWEPAM) [17]. All of the parameters are time-lagged by 54min to include propagation to the subsolar magnetopause.

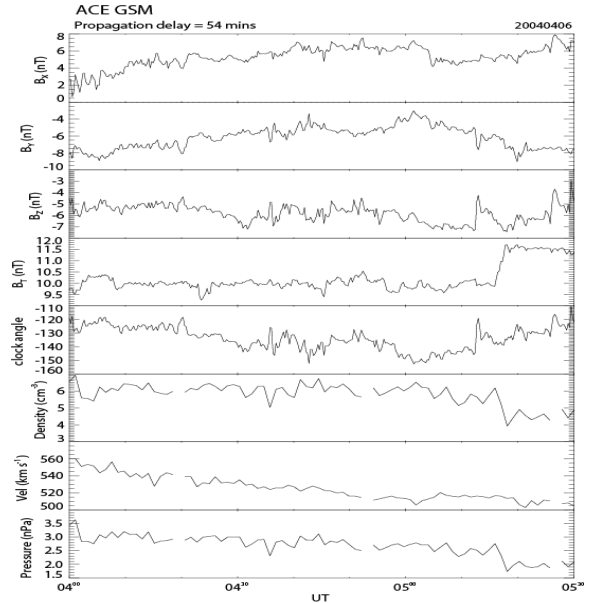


Figure 2. IMF and solar wind conditions on 6th April 2004 from 0400-0530 UT from ACE MFE and SWEPAM instruments. Panels show B field GSM x , y , z and magnitude, IMF clock angle, and solar wind density, velocity and pressure.

The north-south component (B_z) of the IMF varied between -5 and -7 nT, whilst the east-west component (B_y) steadily decreased in magnitude from -8 nT to -4 nT by 0500 UT. From the clock angle, it is clear the field was initially predominately eastward (field angle $\sim 120^\circ$) and then rotated to a more southerly direction ($\sim 150^\circ$) close to 0500 UT. These conditions are favourable for low-latitude subsolar reconnection, with the B_y asymmetry most likely producing a draping of field lines over the magnetosphere as well as the motion of the flux tubes in accordance with the field tension force. The solar wind dynamic pressure was relatively steady at ~ 2 - 3 nPa and the solar wind velocity decreased from ~ 560 km s⁻¹ to 500 km s⁻¹ over the course of the interval.

2.3 Cluster Observations

High time resolution data from EFW [18] and FGM [19] from all four Cluster satellites are shown in Figure 3 in a subset time interval of 0430-0448 UT. The spacecraft are colour coded in the traditional colours and all components are in GSM coordinates. From the top, we have the high time resolution (25Hz) EFW data giving the density (derived from the spacecraft potential (private communication H. Laakso)) the three components of the electric field, and the three components of the drift velocity derived from the electric and magnetic field. Additional care must be employed during the calculation of the drift velocity when the magnetic field is close to the spin plane. The data need to be handled very carefully during these times to ensure that the resulting velocities are realistic.

The bottom four panels show the three components of the magnetic field and the total field strength from FGM at 0.2s resolution.

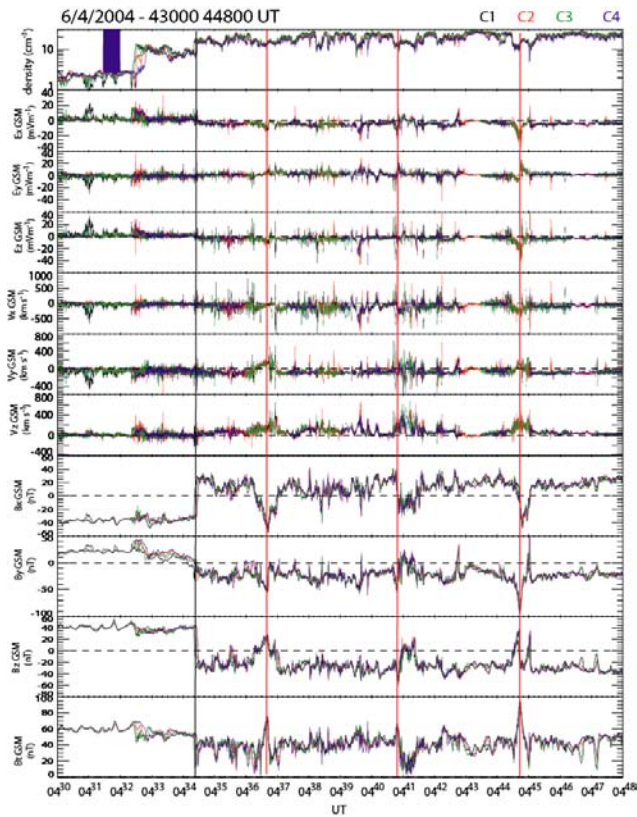


Figure 3. Cluster data from EFW and FGM from 4 spacecraft in GSM coordinates. The top panel is the conversion of spacecraft potential into density, then the 3 compts of electric field and drift velocities. The bottom 4 panels show the magnetic field data in x, y, z directions and field magnitude. The solid black and red lines indicate the magnetopause crossing and transient reconnection signatures, respectively (see text).

The FGM data show clear boundary crossings as well as several transient features identified by the increase in the field magnitude, each of which has been marked with a red line. As the spacecraft passed through the magnetosphere towards the boundary, the field became slightly more turbulent at ~ 0432 UT, though the orientation does not alter. At this time there was a significant jump in the plasma density and an increase in the drift velocity. These features suggest Cluster had crossed into a boundary layer region with a significantly different plasma environment although the field structure was predominately magnetospheric. A couple of minutes later (~ 0434 UT, black line) a clear magnetopause crossing was observed in all parameters, as the field turned to more IMF orientations (see Fig. 1) and the level of turbulence increased suggestive of a compressed magnetosheath field. There was a slight increase in the density at this point also, however not to the same degree as the boundary layer crossing,

implying a certain amount of plasma mixing in the boundary layer region prior to the magnetopause crossing. With the extended period of southward IMF, reconnection processes allowed the influx of magnetosheath plasma into the boundary layer, giving rise to the jump in the plasma density at the earlier time. The following three red lines mark intervals where the magnetic field components indicated magnetospheric field directions, together with a significant increase in the total field strength. Each event also showed a depletion in the plasma density suggesting a mixing of magnetospheric/magnetosheath plasma. The features have been identified as transient reconnection signatures or FTEs from with the mixing of the plasma and field orientations. Additionally, the drift velocities show enhancements of a few hundred km in each of the events. These will be investigated in greater detail below.

To isolate the FTE structures more clearly, the FGM data were rotated into boundary normal coordinates by means of a minimum variance analysis (MVA) [20] on the magnetic field data. This coordinate system, LMN as defined by [7], consists of N pointing outward in the magnetopause boundary normal direction, L lies in the boundary and points northward such that the L - N plane contains the GSM Z-axis, and M also lies in the boundary pointing west to complete the right-handed set. Using this coordinate transformation on the magnetic field data, the transient reconnection signatures were readily identifiable, as shown in Figure 4.

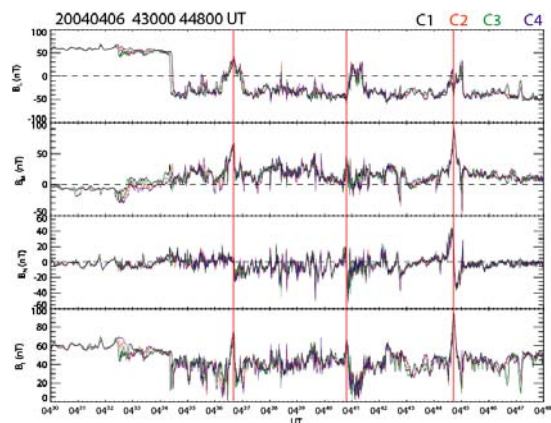


Figure 4. Minimum variance analysis on FGM data to highlight the FTE signatures, marked by red lines.

Each FTE was of a ‘standard’ polarity with a \pm bipolar signature in the normal component (B_N), indicating the passage of a ‘bubble’ of reconnected material over the spacecraft position, and that the reconnection site was located equatorward of the spacecraft. Characteristic increases in the total field strength were also noted in conjunction with the bipolar variations. The other components of the field measured a significant increase of several 10s of nT poleward and westward ($+B_L$ and

$+B_M$) as the FTEs pass over the spacecraft. This is entirely consistent with the motion of newly reconnected flux tubes with a $-B_y$ asymmetry causing the flux tubes to rotate anticlockwise in the plane of the magnetopause, producing a poleward and westward motion in the field, as the flux tubes contract over the spacecraft in time. This effect has previously been observed under positive IMF B_y conditions as Cluster passed through the boundary [21].

Figures 5-7 show the EFW data for each of the FTE events transformed into boundary normal over a 90sec interval spanning the density depletion associated with each signature. The top four panels in each plot show the plasma density and the three components of the electric field. The subsequent panels show vector velocities in the L - M plane (the plane of the magnetopause), M - N plane (looking from above the Earth) and L - N plane. Figure 5 shows the first FTE event between 0436:00-0437:30 UT. The density depletion (top panel) marks the extent of the reconnected material. At the start of the interval the feature passes over the satellite C4 approximately one spin cycle (~ 4 s) before the other 3 satellites. This agrees with the relative locations of the satellites in the L - M plane with C4 being the most equatorward of the four satellites. Prior to the density depletion the electric fields were nominal and the drift velocities indicated a poleward and westward motion of the magnetosheath plasma. At the edge of the newly reconnected flux tube ($\sim 0436:10$ UT), the electric field increased and significant drifts were observed, followed by a rotation in the flow ~ 10 s after the crossing. The velocities showed predominately poleward and westward ($+V_L$, $+V_M$) flows at the edge of the event, representative of magnetosheath plasma motion anti-sunward over the spacecraft with a dawnward rotation. However, within a few spin cycles, the flow weakened slightly and rotated clockwise in the magnetopause dawn-dusk plane to a predominately poleward and slightly eastward direction. Then the drifts intensified in the centre of the event (0436:45 UT) and rotated more rapidly anticlockwise in the L - M plane. The extent of this rapid rotation of the flow was very short lived, and within a few spin cycles the trailing edge of the structure moved over the spacecraft returning the flow to poleward and westward orientations again. The eastward rotation inside the structure can be attributed to the $\mathbf{j} \times \mathbf{B}$ force rotating the newly reconnected field lines in the plane of the magnetopause as they contract duskward over the boundary. Since the ‘exterior’ flow has a dawnward component, a clockwise rotation would be expected such that the plasma would be consistent with flow on newly reconnected field lines. The plasma is dragged along these field lines away from the reconnection site. The internal rotations in the flow suggest some active flow vortices perhaps associated with more recently reconnected material, or some turbulent process due to the mixing of plasma environments. Incidentally, the timing

of the central flow feature corresponds with the peak in the total field strength and the bipolar variation in normal component of the magnetic field (see Fig. 4).

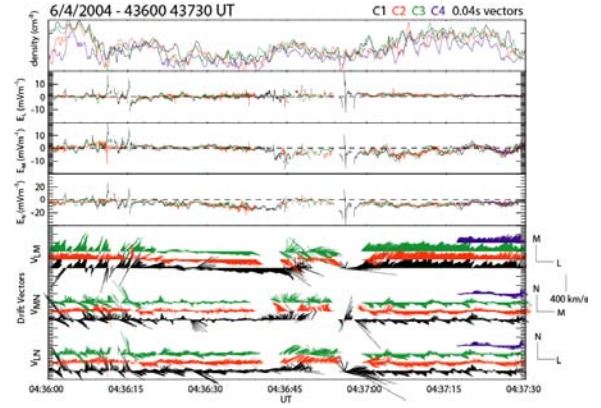


Figure 5. Cluster EFW high-time resolution data (0.04s) transformed in boundary normal coordinates using MVA technique FTE spanning 0436:30UT – 0437:30UT. Panels show the density, electric field in L , M , N directions, and then vector velocities in each of the respective planes, L - M , M - N , and L - N .

Figure 6 shows the second significant reconnection signature identified from the depletion in the plasma density and the bipolar signature in B_N . Again, the time scale covers the 90s interval enclosing the event.

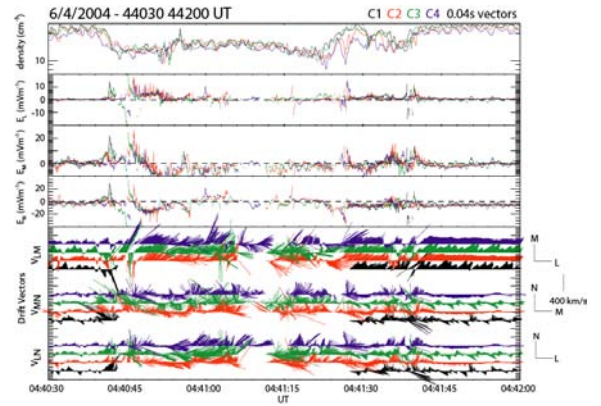


Figure 6. Format as in Fig. 5 for time interval 0440:30UT – 0442:00UT

As in Fig. 5, large electric fields and drift velocities were observed near the edges of the event. In this instance the variations were more turbulent than in the previous case. Immediately inside the event (0440:40 UT), the flow was poleward and westward, similar to the prior case. This was followed ~ 10 s later by a rotation of the flow in the magnetopause dawn-dusk plane in an easterly direction to more poleward orientations. In the central region, the flow turned eastward ($-V_M$), before finally returning to the pre-event flow structure of poleward and westward. Although the drift velocities are far more variable in this event than in the previous, the overall structure and orientation of the

flow was the same. Figure 7, for 0444:00 UT–0445:30 UT, showed a similar flow pattern, although here the rotation was much less turbulent. There was a clear demarcation in the flow of that which occurred inside the event and that which occurred outside. The flow was observed to be calm and ordered both inside and outside the event, with the principal rotation in the magnetopause dawn-dusk plane occurring at the edges of the structure. Poleward and westward flows were observed in the initial stages of the structure (0444:30 UT), followed by an eastward rotation to almost purely poleward orientations (0444:45 UT). This eastern rotation is less obvious in this event, but it is still clear, again indicating the plasma drifting with the field tension associated with newly reconnected flux tubes. At the outer edge, ~0445:00 UT, the flow returned to the poleward and westward direction, as was seen in the other events. In all of the above events, the feature moved poleward over the spacecraft and had rotations in V_N producing vortical structures in the normal direction.

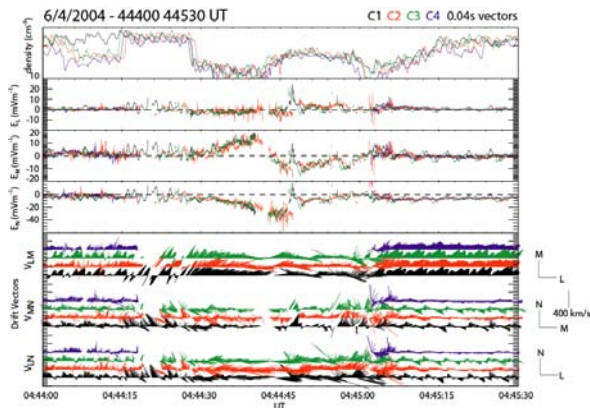


Figure 7. Same format as Fig. 5 for time interval 0444:00 UT – 0445:30 UT.

3. DISCUSSION

The bubbles of reconnected material in each of the cases identified here were enclosed in a background flow that was directed poleward and downward. The downward asymmetry was likely a creation of the magnetosheath plasma moving with the draped field. The magnetic field in the boundary normal coordinates, clearly show the rotation of the field poleward and downward in each of the case, highlighting that there was a rotation in the field structure as the FTE passed over the spacecraft. The field rotation implies the reconnection site moved downward (with $-IMF B_y$ tension effects), skewing the draped field lines accordingly (See Fig. 4). However, the interior of the FTE displayed a flow structure with a significant eastward rotation in the dawn-dusk plane. This could be interpreted as a region containing newly reconnected field lines where the plasma was dragged by the $j \times B$ tension force pulling the plasma duskward away from the reconnection site. The tension force

would produce the eastward rotation in the flow, and since this is only observed in the core of the FTE, the suggestion that this region contains newly reconnected material seems viable. The indication that FTEs can contain these two distinct regions has been present previously, for instance by [22], where the authors were able to identify an outer draped field region and a central core region using plasma and magnetic field data. Here the drift velocities also seem to show some demarcation between the different regions within FTEs.

In an attempt to quantify the difference between the exterior layers and interior region of the FTE, the currents associated with the boundary crossings are investigated using the curlometer technique with the 4 spacecraft FGM data [23]. Each of the three events was investigated with similar results.

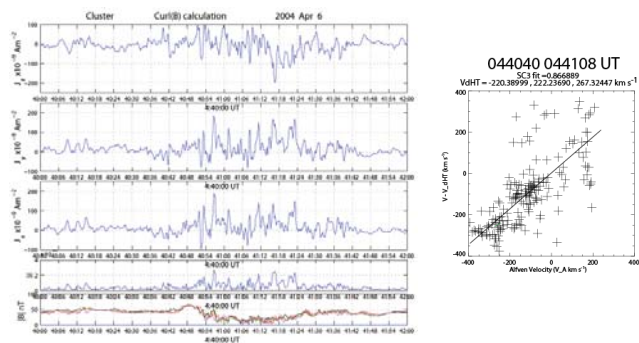


Figure 8. Left panel shows the current determined using the curlometer for time interval 0440 UT – 0444 UT.

The three components of the current, the current magnitude and the field magnetic. Right panel shows the resulting Walen plot for C3 between 0440:40 UT – 0441:08 UT.

Figure 8 (left panel) shows the currents determined for the second event, between 0440 UT – 0442 UT. There appear to be two distinct regions of peak current activity, spanning from 0440:48 UT to 0441:30 UT. This indicated that two separate plasma regimes were sampled and can be distinguished using the currents. This would be expected as the leading edge of the FTE passed over the spacecraft at 0440:45 UT. One current system would give rise to the flow rotation associated with this crossing, and perhaps another with the inner flow regime observed. Comparing the flow in each of these current regions using the Walen Test can bring insight into the nature of the crossing discontinuity. The right panel in Figure 8 shows the corresponding scatter plot of the difference between the drift velocity observed by C3 between 0440:40 UT– 0441:08 UT and de Hoffman Teller velocity in this interval, and the local Alfvén velocity. The successfulness of the Walen test is indicated by the data falling close to the main diagonal, leading to the conclusion that the leading edge of the FTE was a rotational discontinuity.

4. SUMMARY

We present data of three FTE signatures using multi instrument data from Cluster EFW and FGM. Cluster was making a high-latitude outbound pass during an extended period of southward IMF with a significant dawnward component. The FTE signatures were clearly visible in the boundary normal components of the FGM data. Subsequently, the high time resolution EFW data was used to investigate the details of each FTE structures. These data revealed that there were significant drifts poleward and westward at the leading and trailing edges of the FTEs corresponding to the magnetosheath flow in the draped field encapsulating the structures. An eastward rotation was observed immediately inside the FTE structure indicative of $\mathbf{j} \times \mathbf{B}$ tension force pulling the newly reconnected flux tubes away from the reconnection site together with the newly mixed plasma. Further velocity enhancements were observed in the central regions of the FTEs which were likely due to vertical structures and rotations due to the newly reconnected material. The investigation of the current systems within the FTEs highlighted distinct plasma regimes, and by isolating the primary source of plasma of the leading edge of the FTE a clear rotational discontinuity was identified from the Walen test. Further investigation of the internal velocity structures observed in each FTE are underway.

5. ACKNOWLEDGEMENTS

The authors would like to thank the Cluster instrument teams for providing the data and for successful operations for the last 5 years. This work was initiated by the ISSI working group 'Comparative Cluster-Double Star measurements of the Dayside Magnetosphere' under the sponsorship of ISSI, Berne, Switzerland. We would like to thank N.F. Ness at Bartol Research Institute and D.J. McComas at Southwest Research Institute for the use of Level 2 ACE magnetic field (MFE) and ACE solar wind (SWEPAM) data, respectively.

6. REFERENCES

[1] Dungey, J.W., Interplanetary magnetic field and auroral zones, *Phys. Rev. Lett.*, **6**, 47, 1961
 [2] Cowley, S.W.H., Evidence of the occurrence and Importance of reconnection between the Earth's Magnetic Field and the Interplanetary Magnetic Field, *AGU Geophys. Mono.* **30**, edited by Hones, E.W., pp375, 1984
 [3] Gosling, J. *et al.*, Observations of Reconnection of Interplanetary and Lobe Magnetic Field Lines at the High-Latitude Magnetopause, *J. Geophys. Res.*, **96**, 14097, 1991
 [4] Phan, T.D., *et al.*, Extended Magnetic Reconnection at the Earth's Magnetopause from Detection of Bi-Directional Jets, *Nature*, **404**, 848, 2000

[5] Retino, A., *et al.*, Cluster Multispacecraft Observations at the High-Latitude Duskside magnetopause: Implications for Continuous and Component Magnetic Reconnection, *Ann. Geophys.*, **23**, 461, 2005
 [6] Haerendel, G., *et al.*, The Frontside Boundary Layer of the Magnetopause and the Problem of Reconnection, *J. Geophys. Res.*, **83**, 3195, 1978
 [7] Russell, C.T. and R.C. Elphic, Initial ISEE Magnetometer Results: Magnetospheric Observations, *Space Sci. Rev.*, **22**, 681, 1978
 [8] Russell, C.T. and R.C. Elphic, ISEE Observations of Flux Transfer Events, *Geophys. Res. Lett.*, **6**, 33, 1979
 [9] Paschmann, G., *et al.*, Plasma and Magnetic Field Characteristics of Magnetic Flux Transfer Events, *J. Geophys. Res.*, **87**, 2159, 1982
 [10] Saunders, M.A., *et al.*, Flux Transfer Events – Scale Size and Interior Structure, *Geophys. Res. Lett.*, **11**, 131, 1984
 [11] Rijnbeck, R.P., *et al.*, A Magnetic Boundary Signature Within Flux Transfer Events, *Planet Space Sci.*, **35**, 871, 1987
 [12] Thomsen, M. *et al.*, Ion and Electron Velocity Distributions within Flux Transfer Events, *J. Geophys. Res.*, **92**, 12127, 1987
 [13] Owen, C.J. *et al.*, Cluster PEACE Observations of Electrons During Magnetospheric Flux Transfer Events, *Ann. Geophys.*, **19**, 1509, 2001
 [14] Escoubet, C.P., *et al.*, Introduction: the Cluster mission, *Ann. Geophys.*, **19**, 1197, 2001
 [15] Stone E.C., *et al.*, The Advanced Composition Explorer, *Space Science Rev.*, **86**, No. 1-4, 1, 1998
 [16] Smith, C. W., *et al.*, First Results from the ACE Magnetic Fields Experiment, *Space Science Rev.*, **86**, 613, 1998
 [17] McComas, D.J., *et al.*, Solar Wind Electron Proton Monitor (SWEPAM) for the Advanced Composition Explorer, *Space Sci. Rev.*, **86**, 563, 1998
 [18] Gustafsson *et al.* The Electric Field and Wave Experiment for the Cluster Mission, *Space Sci. Rev.*, **79**, 137, 1997
 [19] Balogh, A. *et al.*, The Cluster Magnetic Field Investigation, *Space Sci. Rev.*, **79**, 65, 1997
 [20] Sonnerup and Cahill, Magnetopause Structure and Attitude from Explorer 12 Observations, *J. Geophys. Res.*, **72**, 171, 1967
 [21] Wild, J.A., *et al.*, First Simultaneous Observations of Flux Transfer Events at the High-Latitude Magnetopause by Cluster Spacecraft and Pulsed Radar Signatures in the Conjugate Ionosphere by the CUTLASS and EISCAT Radars, *Ann. Geophys.*, **19**, 1491, 2001.
 [22] Le, G. *et al.*, The Magnetic and Plasma Structures of Flux Transfer Events, *J. Geophys. Res.*, **104**, 233, 1999
 [23] Dunlop, M., *et al.*, Four-point Cluster application of magnetic field analysis tools: The Curlometer, *J. Geophys. Res.*, **107**, doi: 10.1029/2001JA005088, 2002